2014 IEEE International Conference on Robotics & Automation (ICRA)
Hong Kong Convention and Exhibition Center
May 31 - June 7, 2014. Hong Kong, China

An Intuitive Multimodal Haptic Interface For Teleoperation of Aerial Robots

Xiaolei Hou, Robert Mahony

***Abstract*— This paper presents a novel intuitive multi-modal force feedback interface for teleoperation of mobile robotic vehicles. Two different force feedback interfaces are considered: a force feedback joystick and a novel force feedback trackball. The joystick considered is based on the admittance user interface developed by the authors in earlier work and is configured to servo velocity of the vehicle. The force feedback trackball is configured to map vehicle velocity directly to trackball velocity, exploiting the effectively infinite workspace of the trackball to overcome the classical challenge of servo controlling a slave with infinite workspace using a master device with finite workspace. A key contribution of the paper is to provide a modeling framework, based on the bond graph formalism, that allows the energy consistent modeling of input from an admittance joystick as reference to an internal velocity regulation loop for the vehicle. Once this is implemented it is straightforward to interconnect multiple input devices, and in particular the trackball device, using standard interconnection rules in bond graphs. Experiments were performed, and the outcomes verify the feasibility and effectiveness of the proposed interface.**

I. INTRODUCTION

Mobile robot teleoperation has been an active research area since the late 1990s [10], [9]. Force feedback has been verified to be effective in assisting pilots to avoid collisions with scattered obstacles in the environment [16], [13], [11]. Environmental information is typically reflected to the users as an exogenous force applied to the slave robot [16], [5]. A diverse range of force cues have been investigated in the literature and the outcomes indicate that obstacle avoidance algorithms containing a velocity-over-distance term generally have better performance in preventing collisions [2], [17], [13]. With assistance of this environmental force feedback, pilots can better avoid collisions or near collisions in the environment [17], [13], and thus better perform the navigation tasks for the mobile robots. The large (effectively infinite) workspace of a mobile robot, however, precludes the standard position-to-position (P2P) forward mapping between master and slave used in manipulator teleoperation. A position-to-velocity (P2V) mapping is widely used and is well adopted to achieve unlimited workspace for the slave robots [26], [21], [12], although such an approach naturally leads to less precise position control. In [6], a hybrid approach is proposed that switches between P2P and P2V mapping depending on the robot's distance to the obstacles and master joystick's speed. Schill *et al* [21] introduced a leaky integrator concept that seamlessly integrates the P2V mapping with P2P mapping. The leaky integrator is implemented in the position controller of master joystick that is configured under admittance mode, and estimates an approximated user force input to control vehicle continue moving. In [20], a scrolling-based approach is proposed that allows the user to scroll through the slave's workspace and reset the master's workspace using a button on master device. A workspace drift control approach is proposed by Conti [3] to reset the centre of slave workspace when the user touches the boundary of the workspace. A similar approach is used by Omari *et al.* [19].

Passivity analysis provides a powerful framework to analyze robustness and stability of bilateral force feedback teleoperation systems [15], [22], [26]. An energetically consistent model of bilateral force feedback also makes interconnection of multiple input devices straightforward [8], [24], [14]. However, the mismatch of the state correspondence between a joystick input master device and mobile robotic slave vehicle for P2V architectures means that energetic modeling of the resulting bilateral force feedback coupling is not straightforward. As a consequence, there is no existing framework available to model bilateral force feedback of mobile vehicles in an energy consistent manner. This is particularly important when it is desired to interconnect multiple master devices to address issues associated with providing accurate position control (provided by a P2P master device) while maintaining good control of velocity in an infinite workspace (provided by a P2V master device).

In this paper, we propose an energy consistent framework for modeling bilateral teleoperation of mobile robotic vehicles. The framework developed will allow us to connect multiple input devices in a straightforward manner, and we demonstrate this by interconnecting an admittance master joystick (P2V) and separate master trackball (P2P) to pilot a quadrotor vehicle. The approach is based on the bond graph modeling framework and makes use of a gyrator element. Energy for the internal velocity control of the vehicle is provided by an internal storage element and a general Dirac structure that allows the implementation of arbitrary control laws. The proposed system framework has some similarities to the PSPM framework proposed by Lee [14]. The energetic passivity for the system can be easily obtained to ensure the stable interaction between master and slave system. The proposed framework is capable of integrating multiple force feedback devices offering diverse force feedback cues to human operator for better understanding of the situation.

The remainder of the paper is organised as follows. Section II provides problem formulation. The proposed system architecture and analysis are given in Section III. Simulation

Xiaolei Hou and Robert Mahony are with Research School of Engineering, Australian National University, Canberra, ACT 0200, Australia xiaolei.hou, robert.mahony@anu.edu.au

and experiment data is presented and analyzed in Section V. Section VI concludes the paper.

II. PROBLEM FORMULATION

A. Mobile Robot Control

Although the full dynamics of a mobile robotic system can be complex [12], [15], when taken in closed loop with a suitable low level attitude/motor regulation, simple point mass dynamics typically provide a good model

$$M_{\rm s}\dot{v}_{\rm s} = f_{\rm s}, \tag{1}$$

where $v_s \in \mathbb{R}^3$ is the slave vehicle velocity, $M_{\rm s}$ is a scalar mass and $f_{\rm s} \in \mathbb{R}^3$ denotes the force control. In the case of aerial robotic systems, an inner control loop not modeled in the teleoperation architecture, is associated with the high gain regulation of the vehicle attitude and compensation for gravity. The associated vehicle kinematics are

$$\dot{x}_{\rm s} = v_{\rm s}. \tag{2}$$

The slave vehicle is typically also provided with an additional velocity control loop with reference set point derived from signals provided by the pilot. We choose to include a model of the velocity regulation control loop as part of the teleoperation architecture since it is fundamental in converting the system inputs, as seen by the master control system, from force like objects $f_{\rm s}$ in (1) to velocity references v_r. In most cases, and since exact tracking of the reference velocity is not required when the reference velocity is provided in real time by a pilot, the velocity regulation loop can be implemented as a simple proportional feedback

$$f_{\rm s} = -k(\dot{x}_s - v_{\rm r}). \tag{3}$$

More sophisticated velocity regulation control is not precluded by the modeling approach proposed in this paper, however, in all cases the resulting control system will require physical energy to implement. Since the proposed teleoperation scheme is fundamentally constructed based on energetic principles, keeping track of the energy balance of the internal velocity regulation is a critical part of the proposed closed-loop architecture.

B. Force Feedback Joystick

There are two types of configurations that can be considered for a master force feedback joystick: impedance or admittance configured user interface. Impedance configured user interfaces are by far the most common joystick configuration and there are very few commercially available force feedback joysticks with admittance configured user interface. A typical impedance configured force feedback joystick, such as Force Dimension Omega series [4], is a low inertia, low friction and back drivable device that measures the position of the end-effector and exerts force and torque to human user. An admittance configured joystick has high inertia, high friction and is not back-drivable, for example the HapticMaster [25] and ANU admittance joystick [11]. Such a joysticks are equipped with force sensors that measure the input force applied by the user and are actuated by stepper motors or other position servo devices that are agnostic to back force applied by the pilot.

Both admittance and impedance configured master joysticks are dynamical systems and could be modeled in the control architecture. However, both systems have significant internal control actuation and are built to minimize the effect of the internal dynamics on the way in which the device interacts with the environment. As such it is acceptable to consider the joystick devices as pure input-output devices: admittance devices that accept a force and servo position, and impedance devices that accept position and servo force. Both devices, however, will be actuated by the same human operator. This is possible due to the natural compliance of a humans in manipulating physical objects. When interacting with an impedance device, the forces applied by the joystick device are insufficient to significantly displace a human arm and the pilot acts to servo position of the joystick. In the terminology of bond graphs, the human acts as a source of flow $\mathbf{Sf}$. When interacting with an admittance device, the human muscles still act as though to move the arm to a desired position, however, due to the stiffness of the end effector of the joystick, the forces applied by the muscles are absorbed into the natural mechanical compliance of the arm. In this case the pilot acts to apply a force to the end effector of the joystick. In the terminology of bond graphs, the human acts as a source of effort $\mathbf{Se}$.

Humans perceive force both through tactile sensations in the fingers and hand and through kinetic sensations in the arm itself. In the case of an impedance joystick, this sensation is then the primary sensory feedback from the interaction, while in the case of admittance, this becomes an internal signal that is in effect the signal that the user regulates to achieve the teleoperation goal.

C. Force Feedback Trackball

The force feedback trackball is an ideal master device to provide partial P2P control of a slave moving in a workspace with two infinite degrees of freedom. The continuous rotational motion of trackball can encode infinite workspace in the horizontal plane for mobile robots by mapping pitch and roll of the ball to displacement in the x and y directions in the plane. To intuitively perceive the motion of the slave robot, the trackball is configured as an admittance force feedback device that servo controls the pitch and roll angular velocity of the trackball to match x and y velocity of the robot, while measuring torque applied to the trackball by the pilot.

The state of the trackball lives in $\mathrm{SO}(3)$ with velocity $\Omega \in \mathbb{R}^3$ and kinematics

$$\dot{R} = \Omega_\times R. \tag{4}$$

Here, Ω denotes the angular velocity of the trackball in the inertial frame, corresponding to the trackball base structure.

The trackball developed at ANU has only two axes of rotation actuated, the x- and y-axes, corresponding to lateral and forward rotation of the trackball respectively. The third axis, rotation around the vertical axis, is prevented by the physical actuation mechanism of the ball. The motors are deliberately high torque, high bandwidth actuation with velocity control and current measurement. The inertial frame torques are estimated by measuring and modeling current flow in the drive motors. A zero-payload current-velocity model is established to estimate the human force inputs.

III. Energy consistent modeling of velocity controlled teleoperation

Integrating multiple different force feedback devices into a single system architecture requires one to use an underlying modeling framework. The port Hamiltonian framework has proved to be an ideal framework for interconnection of mechanical subsystems in an energy consistent manner [23], [24]. The classical formulation of bilateral force feedback systems in the port Hamiltonian framework is formulated for P2P configuration systems. The port Hamiltonian framework can be applied directly to the trackball system, however, it requires careful consideration in order to apply the same concept to the P2V joystick master devices. In this section, we show how a port Hamiltonian modeling framework can be adopted for both the joystick configurations and the trackball system in ideal conditions. A more sophisticated architecture is introduced in the next section to deal with non-ideal situations. We will use the bond graph graphical notation to provide a clear schematic architecture of the interconnection structure.

A. Force Feedback Trackball

Recall the discussion of the trackball given in §II-C. In order to interconnect this system to the vehicle dynamics we begin by assigning a mapping between slave velocity and master trackball velocity

$$\Omega_y = -\mu v_x, \qquad \Omega_x = \mu v_y. \tag{5}$$

for $\mu > 0$ a scaling factor. This relationship maps scaled planar velocity of the vehicle to angular velocity of the trackball such that the linear velocity of the top of the trackball corresponds to the motion of the vehicle, the most intuitive motion correspondence for the pilot. The scaling factor $\mu > 0$ is included to provide a means to tune the sensitivity of the trackball response. The above relationship can be written as a matrix relationship

$$\Omega = \mu \begin{pmatrix} 0 & 1 & 0 \\ -1 & 0 & 0 \end{pmatrix} v_{\mathrm{s}} =: \mu M v_{\mathrm{s}}. \tag{6}$$

We define the dual relationship between forces and torques

$$f_{\mathrm{t}} := \mu \begin{pmatrix} 0 & -1 \\ 1 & 0 \\ 0 & 0 \end{pmatrix} \tau = \mu M^\top \tau. \tag{7}$$

where τ is the inertial frame torque applied to the trackball. That is the inertial frame torques τ applied to the trackball are mapped to physical forces in the x-, y-axes of the slave vehicle. The relationships, (6) and (7), define a transformer element in the language of bond graph. That is an energy consistent transformation between system variables. In particular, the mechanical power in the variables f_{t} and v_{s} is equal to the mechanical power in the variables τ and Ω:

$$\langle f_{\mathrm{t}}, v_{\mathrm{s}} \rangle = \langle \tau, \Omega \rangle.$$

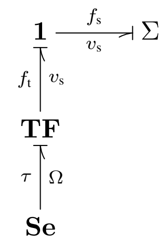

Fig. 1. Direct interconnection of trackball with point mass vehicle dynamics. The bonds indicate dual pairs of effort and flow variables whose inner product is mechanical power. The top bond between the $\mathbf{1}$ junction and the system Σ implements the robot dynamics.The $\mathbf{1}$-junction is a force summing junction that will be used as the point to interconnect the different user interface devices. The transformer $\mathbf{TF}$ implements the relationships (6) and (7).

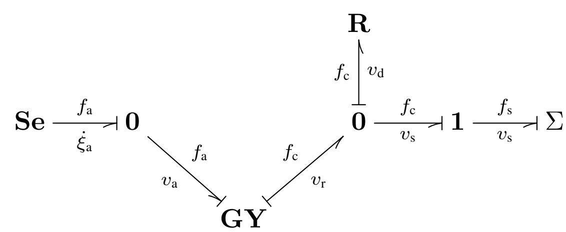

Fig. 2. System architecture for an admittance joystick in P2V configuration with simple damping injection velocity control. The gyrator allows the force applied by the user to be converted into a velocity reference while at the same time reflecting the system dynamics to generate the desired velocity tracking reference for the master servo position.

In the notation of bond graph, we have the interconnection shown in Figure 1. The $\mathbf{1}$-junction is unnecessary for the this simple structure, however, it will act as the attachment point for the multiple input devices.

B. Admittance Joystick

The second situation that we consider is the interconnection of an admittance joystick with the physical system Σ. In this case, we need to model the P2V nature of the reference signal. In order to do this it is necessary to model the internal velocity control loop of the slave mechanism. In this section we will consider a simple proportional type control (3) that can easily be provided with an explicit port Hamiltonian implementation. More sophisticated control actions can be considered using the formalism introduced in §IV.

Consider the bond graph shown in Figure 2. The system model at the right-hand side is just the implementation of (1) and the $\mathbf{1}$-junction is left in place for future interconnections of multiple input devices. The $\mathbf{0}$-junction on the left of the $\mathbf{1}$-junction is a velocity summing junction. The velocity in the lower left bond v_{r} is the reference velocity, the velocity in the right bond v_{s} is the slave velocity, and one has that

$$v_{\mathrm{d}} = v_{\mathrm{r}} - v_{\mathrm{s}} \tag{8}$$

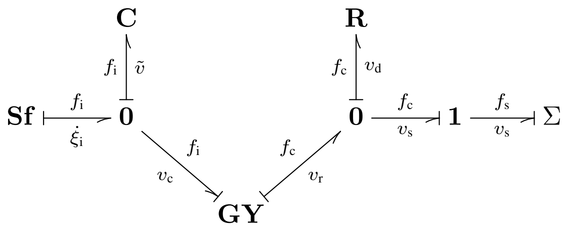

Fig. 3. System architecture for an impedance joystick in P2V configuration with simple damping injection velocity control. The architecture is the same as the admittance case Figure 2 except for the additional spring storage element $\mathbf{C}$ that allows the joystick to move and reflects offset force back to the pilot.

is the tracking error. The damping control is provided by the impedance $\mathbf{R}$ that assigns the force

$$f_\mathrm{c} := R(v_\mathrm{r} - v_\mathrm{s}) \tag{9}$$

for $R > 0$ the damping constant.

The remainder of the bondgraph is the structure that allows for implementation of the P2V control signal. The gyrator element $\mathbf{GY}$ implements the dual relationship

$$v_\mathrm{a} := \frac{\gamma}{M_\mathrm{s}} f_\mathrm{c}, \qquad v_\mathrm{r} := \frac{\gamma}{M_\mathrm{s}} f_\mathrm{a} \tag{10}$$

where $\gamma > 0$ is a positive scaling factor. From this relationship we see directly that the velocity reference v_r for the vehicle control system is a scaled version of the force applied to the admittance joystick. Moreover, the position of the joystick is given by the kinematics

$$\begin{aligned}\dot{\xi}_\mathrm{a} = v_\mathrm{a} &= \frac{\gamma}{M_\mathrm{s}} f_\mathrm{c} = \frac{\gamma}{M_\mathrm{s}} M_\mathrm{s} \ddot{x}_\mathrm{s} \\ &= \gamma \ddot{x}_\mathrm{s}\end{aligned}$$

where we substitute (1) for the force $f_\mathrm{c} = f_\mathrm{s}$. Thus, one has

$$\xi_\mathrm{a} = \gamma \dot{x}_\mathrm{s}, \tag{11}$$

where we assume in addition that $\xi_\mathrm{a}(0) = \dot{x}_\mathrm{s}(0)$, that is that the system is suitably initialized. This implements the desired scaled velocity position feedback for an admittance master device, that is the master device position is servo controlled to the slave velocity.

C. *Impedance Configured Force Feedback Joystick*

The final scenario we consider is that of an impedance configured force feedback joystick, Figure 3. In this case the human pilot is modeled as a source of flow $\mathbf{Sf}$ and the system needs to have an element that provides the force mapping that is implemented by the impedance joystick device. The force on the device is provided by a spring element $\mathbf{C}$. The internal spring variable is

$$\zeta = \int \tilde{v} \mathrm{d}t = \int (\dot{\xi}_\mathrm{i} - v_\mathrm{r}) \mathrm{d}t = \int (\dot{\xi}_\mathrm{i} - \gamma \ddot{x}_\mathrm{s}) \mathrm{d}t = \xi_\mathrm{i} - \gamma \dot{x}_\mathrm{s} \tag{12}$$

for suitable initial conditions. If we assign a spring constant $k > 0$ and storage function $H_C = \frac{k}{2}\zeta^2$ then the force f_i that is generated by the system is

$$f_\mathrm{i} := k\zeta = k(\xi_\mathrm{i} - \gamma \dot{x}_\mathrm{s}) \tag{13}$$

That is the force reflected to the user is the offset of the scaled slave velocity to the joystick position. This is the standard choice of reflected force for an impedance joystick configuration [18], [1]. It is interesting to note that the resulting velocity reference is also linked to the restoring force generated by the spring, and hence is a scaled version of the difference $(\xi_\mathrm{i} - \gamma \dot{x}_\mathrm{s})$. The standard assignment of master position to reference velocity used in the literature [13], [7], [1] is $v_\mathrm{r} := k\xi_\mathrm{i}$ for some scaling $k > 0$. The difference seen here is a consequence of the energy consistent modeling of the interconnection. Although we do not undertake comparative experiments in this paper it is arguable that the impedance interconnection proposed here could provide a better feel for the vehicle dynamics than is provided by the standard interconnection that is known to be poor at representing vehicle motion [12]. The standard assignment can be recovered from the more general development presented in the next section by suitable choice of the correction signal w_2 (Figure 5) if required.

IV. A General Construction for Energy Consistent Interconnection of Input Devices for Velocity Control of Mobile Vehicles

The material developed in the Section §III shows how P2V force feedback joysticks can be interconnected with a velocity controlled dynamic system. The analysis given in that section showed only a single interconnection. There are a number of issues that arise when multiple input devices are interconnected and this framework is used in a real world scenario. The key issue is that the position tracking of the joystick, $\xi_\mathrm{a} = \mu \dot{x}_\mathrm{s}$ in the case of the admittance joystick, and $\zeta = \xi_\mathrm{i} - \dot{x}_\mathrm{s}$ in the case of the impedance joystick, depend on integration of the system dynamics model. Even in the ideal case, in any real system this integration will be imperfect, the system forces will be imperfectly modeled, and these relationships will drift if they are explicitly implemented. More importantly, this model depends on reflecting the complete input force applied to the system and when multiple input devices are implemented only the part of the slave force due to that particular device will be reflected through the gyrator link. Thus, in order to implement an interconnection of multiple input devices we will need an architecture that compensates for this mismatch. We will take the opportunity to provide a general structure for implementation of the velocity controller at the same time.

We demonstrate the modified design in the case of the admittance joystick. Consider Figure 4. The human pilot is modeled as source of effort $\mathbf{Se}$ and slave robot dynamics are denoted as $\mathbf{\Sigma}$ as before. The lower branch of the bond graph with the gyrator replicates the structure in Figure 2. The bondgraph is modified to include a Dirac structure $\mathbb{D}$ with a energy storage $\mathbf{C}$ attached in upper branch of the bondgraph. The Dirac structure is a general energy routing unit that can assign signals as required as long as it instantaneously balances energy

$$\langle f_\mathrm{store}, v_\mathrm{store} \rangle = \langle f_\mathrm{c}, v_\mathrm{d} \rangle - \langle f_\mathrm{a}, w \rangle. \tag{14}$$

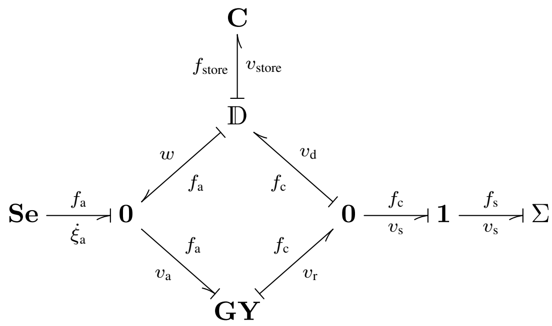

Fig. 4. A general architecture for connection of an admittance configured force feedback joystick for velocity control of mobile robotic system. The upper bondgraph branch provides a mechanism to implement arbitrary velocity controllers and balance energy across the system.

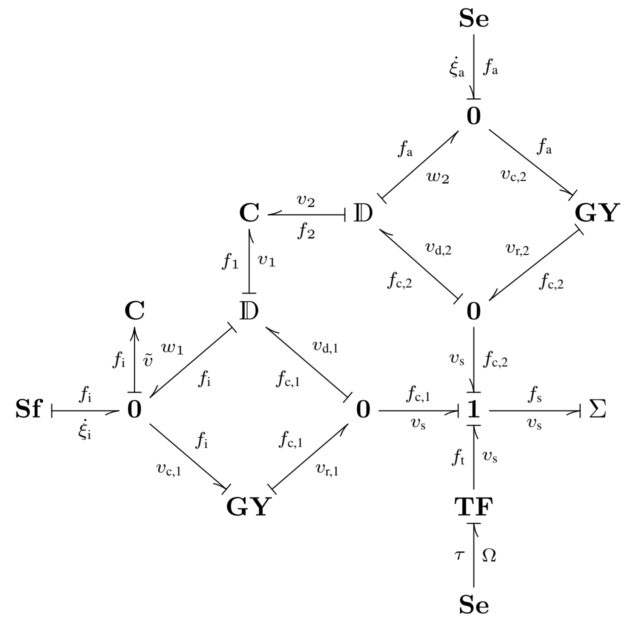

Fig. 5. Interconnection of three different input devices, an impedance configured force feedback joystick (on the left), an admittance configured force feedback joystick (upper right) and an admittance configured force feedback trackball (lower right). The two joysticks share the same storage element for their Dirac structures ensuring that if the energy decreases to zero then both joysticks operate in their basic modes at the same time. This also allows trading of energy between the systems in a natural manner. Since trackball is a direct force connection it does not require an energy storage.

We use the flexibility of this structure to assign any desired velocity control f_{c} and any correction signal w as required. The energy required to achieve this assignment is drawn from the store $\mathbf{C}$ until this store is empty. If the energy store runs down to zero then we will either assign $f_{\text{c}} = 0 = w$ if the desired inputs requires energy from $\mathbf{C}$, or implement the desired signals if they replenish the energy in $\mathbf{C}$.

The velocity control f_{c} could be a dissipation element as was considered in Figure 2, however, now the energy that was dissipated by this control is stored in $\mathbf{C}$ and can be reused to modify the response of the joystick. Since a stable velocity controller will in general be dissipative, this is the normal scenario that will be encountered, even for a more sophisticated control system.

The signal w is a velocity signal that modifies the joystick reference position kinematics

$$\dot{\xi}_{\text{a}} = v_{\text{a}} - w. \tag{15}$$

This signal is used to servo the master joystick position to ensure that $\xi_{\text{a}} = \mu \dot{x}_{\text{s}}$. In the ideal case where there is only one input device connected and the system dynamics are perfectly modeled, then this correction signal will be zero. In a real world situation then the energy dissipated by the velocity control will certainly be recycled to maintain good tracking of the desired reference position.

The general architecture for the impedance joystick is implemented in a similar manner to that shown for the admittance joystick. The control $\mathbf{R}$ element is replaced by a Dirac structure with a back interconnection to the input $\mathbf{0}$-junction. The architecture is seen in left branch of Figure 5.

A. Interconnection of multiple input devices

Once the general architecture of single input device has been determined, the interconnection of multiple devices is straightforward. The $\mathbf{1}$-junction directly connected to the system is used as a force summing junction. Figure 5 shows the interconnection of three input devices, an impedance configured force feedback joystick (on the left), an admittance configured force feedback joystick (upper right) and an admittance configured force feedback trackball (lower right). The input device subsystems are largely independent of each other, except that we have chosen to have the two joysticks share the same storage element for their Dirac structures. This allows the two subsystems to share energy in a natural manner. In particular, if one of the joysticks is consuming energy to maintain tracking of the joystick reference position then it is likely that this is due to interaction with the other joystick and the energy flow between the two joysticks will ensure minimal depletion of the storage element attached to Dirac structure. The trackball does not store energy and this system can be used to dissipate, or accumulate, energy in the system as required.

The input subsystems interact through the $\mathbf{1}$-junction. All input subsystems experience the same velocity feedback from the system and since their forces are summed they will experience natural force balance coupling. That is if one joystick is used to try and accelerate the vehicle, while the second joystick is used to decelerate the vehicle the two joysticks will ‘feel’ each others force inputs while the system experiences no overall force input. In principle it is possible for the multiple input devices to fight against each other, however, the intuitive interface proposed should ensure that the such a situation is clear to the pilot who may indeed be choosing to play one interface off against another to maintain precise control.

The most common configuration will be the interconnection of a trackball device with a force feedback joystick. This allows the joystick to be used for driving the vehicle while the trackball is used to moderate the motion of the vehicle.

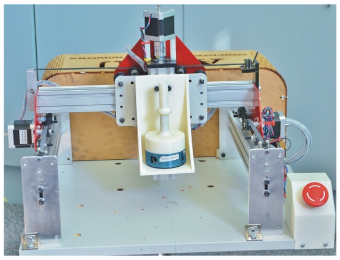

Fig. 6. Admittance force feedback joystick

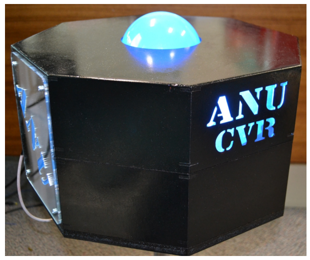

Fig. 7. Track ball

V. EXPERIMENT

In this section, we present results of experiments conducted with a custom admittance configured force feedback joystick [12] and a custom force feedback trackball. The experiment is designed to verify the concept of the proposed framework and its feasibility of implementation.

A. Experiment facility

The experiment was conducted on a robotic platform based on a Mikrokopter quadrotor equipped with onboard vision system flying in a VICON tracking enclosure. The VICON tracking system provides 200Hz position and attitude measurement for regulating vehicle's velocity while the vision subsystem is used purely to provide the pilot with visual feedback. An internal attitude control is present on the vehicle that tracks a desired heading, pitch and roll. Along with thrust control, this leads to a point mass model for the remaining linear degrees of freedom of the aerial robotic vehicle. The aerial vehicle is controlled through a base station over a wifi link and all communications are sufficiently fast that time delays need not to be considered.

Two force feedback input devices are considered in this experiment. Firstly, a custom admittance configured force feedback joystick shown in Figure 6 was used. This joystick is based on a stiff x-y-z off-the-shelf CNC machine base provided with servo control stepper motor positioning. A custom joystick is mounted on a JR3 force sensor from which the x-y-z linear forces are used as control signals for vehicle. The z axis torque is also used to servo vehicle orientation. This joystick input device has been shown to lead to better performance when compared to a traditional impedance configured joystick for control of aerial vehicles [12].

An admittance configured force feedback trackball was developed for this experiment, Figure 7. The trackball is provided with two velocity controlled high torque motors connected to rubber drive wheels that are pressed to the trackball by a passive spring systems. The instantaneous current in each motor is measured and used to estimate torque applied to the trackball. The drive wheels are mounted on the x and y circumference of the ball and actuate pitch and roll motion of the ball in the inertial frame. Yaw motion of the ball is prevented by the rolling non-slipping constraint of the drive wheels.

B. Experiment results

In the experiment undertaken, the pilot was required to command the vehicle to a designated zone in front of a target and stabilized the vehicle. The pilot then engaged in a number of simple manoeuvres designed to test the interaction of the controls. The results are shown in Figure 8, the upper graph showing velocities in the x-axis while the lower graph shows velocities in the y-axis. The red trace is the velocity of the vehicle as measured by the VICON system. Note that the black trace of the trackball angular velocity Ω (with suitable scaling factors) tracks the vehicle velocity exactly. This is a consequence of the one-to-one mapping of velocities that comes with the P2P matching for the trackball. The position of the admittance joystick, shown in green, tracks the vehicle velocity with a small lag due to limitations of the servo control system. The admittance joystick input is traced in blue. This input is acting as a force input to the velocity dynamics. The phase shift of roughly $\pi/4$ is a consequence of the system gain employed in the control. The higher the gain the closer the tracking is expected to be, but also the more sensitive the system is. The pink trace indicates the input force applied to the trackball derived from torque estimate of the trackball drives.

Initially during the flight (0-35s) only the admittance joystick was actively used. After taking off, the vehicle was deliberately manoeuvred from side to side to excite the control actuation. During the period from 40-50 the trackball was used in addition to the joystick input to damp extreme motion of the system and help control the excess sideways motion. In the period from 50-60 and 65-75 seconds the joystick was released, setting the joystick reference velocity to zero. (The period 60-65 seconds the joystick was used to bring the vehicle back into the main flight area after it drifted). During this period the joystick control acts as a damping control on the systems velocity and the trackball provides an input force to control the vehicle. Finally, during the period 80-95 seconds the joystick and trackball were used against each other to get a feel for the force interaction between the devices. The final 5 seconds are used for repositioning the vehicle using the joystick only during the landing sequence. Yaw orientation and z-axis velocities are not plotted since trackball does not control these two Degrees of Freedom.

Overall, the feel of both devices was found to be direct and intuitive. The interaction of the two devices was easily perceived by the pilot. The test pilot found that the most effective control strategy was to use the joystick to actively move the vehicle in a desired direction and then damp that motion using the trackball. The interaction of the two input devices allowed the pilot to regulate the response of vehicle to an input force applied by the joystick immediately by damping using the trackball. Although no detailed comparative user experiments have been undertaken the it appears clear that the proposed architecture leads to a highly effective user interface for teleoperation of aerial vehicles.

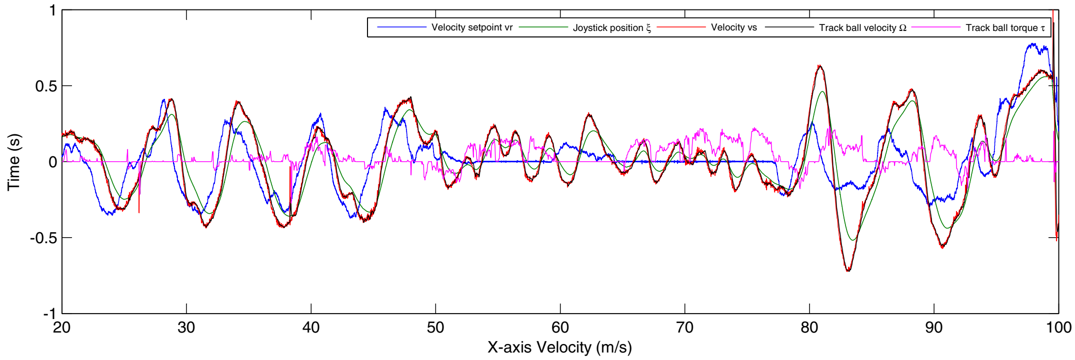

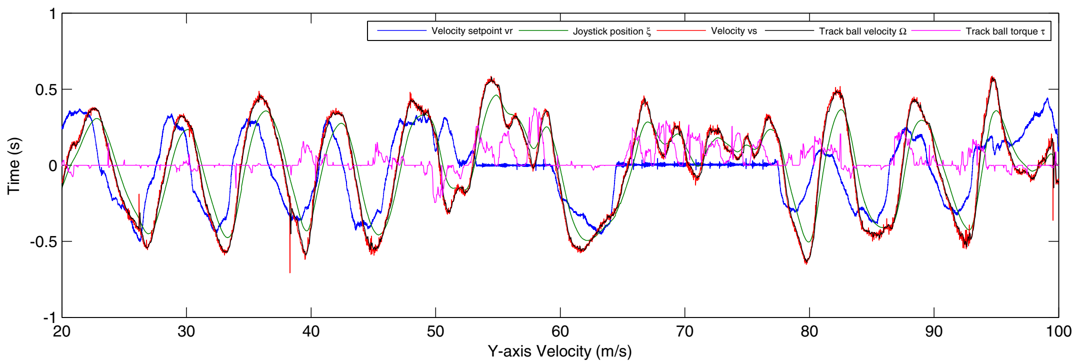

Fig. 8. Experimental results if interconnection of admittance configured joystick and admittance configured trackball input devices

VI. CONCLUSIONS

This paper presents an energy consistent architecture for interconnection of multiple force feedback input devices. An explicit model was given for interconnection of position to velocity control in a bond graph formalism, to the authors knowledge, the first such architecture that has been provided. The general form of this architecture allows interconnection of multiple force feedback input devices in a natural manner. Explicit models for interconnection for both admittance configured and impedance configured force feedback joysticks were provided, as well as the direct interconnection model for a force feedback trackball. To demonstrate the theory, a force feedback trackball was developed and interconnected with an admittance configured force feedback joystick. The results demonstrate that the proposed architecture leads to a stable and effective interface for teleoperation of aerial vehicles.

VII. ACKNOWLEDGMENTS

This research was supported by the Australian Research Council through Future Fellowship FT0991771 Foundations of Vision Based Control of Robotic Vehicles. The authors acknowledge the input of Felix Schill into the conceptual foundation of the paper and would like to thank Alex Martin for developing the trackball platform.

REFERENCES

[1] Mersha. A.Y., X. Hou, R. Mahony, S. Stromigioli, Corke. P., and C. Raffaella. Intercontinental haptic teleoperation of a flying vehicle: A step towards real-time applications. In *Proc. 2013 IEEE/RSJ Int. Conf. Intell. Robots Syst.*, Nov. 2013.

[2] A.M. Brandt and M. B. Colton. Haptic collision avoidance for a remotely operated quadrotor uav in indoor environments. In *Proc. 2010 IEEE Int. Conf. Syst. Man Cybern.*, pages 2724 –2731, oct. 2010.

[3] F. Conti and O. Khatib. Spanning large workspaces using small haptic devices. In *Proc. 1st Joint Eurohaptics Conf. and Symp. Haptic Interfaces for Virtual Environment and Teleoperator Syst., World Haptics Conf.*, pages 183 – 188, march 2005.

[4] Force Dimension. `http://www.forcedimension.com/`.

[5] N. Diolaiti and C. Melchiorri. Teleoperation of a mobile robot through haptic feedback. In *Proc. 2002 IEEE Int. Workshop Haptic Virtual Environments and Their Applications*, pages 67 – 72, 2002.

[6] I. Farkhatdinov and J. H. Ryu. Hybrid position-position and position-speed command strategy for the bilateral teleoperation of a mobile robot. In *Proc. 2007 Int. Conf. Control, Autom. Syst.*, pages 2442 –2447, oct. 2007.

[7] Antonio Franchi, Cristian Secchi, Hyoung Il Son, Heinrich H. Bulthoff, and Paolo Robuffo Giordano. Bilateral teleoperation of groups of mobile robots with time-varying topology. *IEEE Trans. on Robot. and Autom.*, 28(5):1019–1033, 2012.

[8] B. Hannaford and J.H. Ryu. Time-domain passivity control of haptic interfaces. *IEEE Trans. on Robot. Autom.*, 18(1):1–10, 2002.

[9] S. G. Honga, J. J. Lee, and S. Kim. Generating artificial force for feedback control of teleoperated mobile robots. In *Proc. 1999 IEEE/RSJ Int. Conf. Intell. Robots Syst.*, volume 3, pages 1721–1726 vol.3, 1999.

[10] S.G. Honga, B.S. Kim, S. Kim, and J.J. Lee. Artificial force reflection control for teleoperated mobile robots. *Mechatronics*, 8(6):707 – 717, 1998.

[11] X. Hou and R. Mahony. Dynamic kinesthetic boundary for haptic teleoperation of aerial robotic vehicles. In *Proc. 2013 IEEE/RSJ Int. Conf. Intell. Robots Syst.*, Nov. 2013.

[12] X. Hou, R. Mahony, and F. Schill. Representation of vehicle dynamics in haptic teleoperation of aerial robots. In *Proc. 2013 IEEE Int. Conf. Robot. and Autom.*, pages 1447–1483, may 2013.

[13] T. M. Lam, H. W. Boschloo, M. Mulder, and M. M. van Paassen. Artificial force field for haptic feedback in uav teleoperation. *IEEE Trans. Syst. Man Cybern. A., st. Humans*, 39(6):1316 –1330, nov. 2009.

[14] D. Lee and K. Huang. Passive-set-position-modulation framework for interactive robotic systems. *IEEE Trans. on Robot.*, 26(2):354 –369, april 2010.

[15] D.J. Lee, O. Martinez-Palafox, and M.W. Spong. Bilateral teleoperation of a wheeled mobile robot over delayed communication network. In *Proc. 2010 IEEE Int. Conf. Robot. and Autom*, pages 3298–3303, 2006.

[16] S. Lee, G. S. Sukhatme, G. J. Kim, and C. M. Park. Haptic control of a mobile robot: a user study. In *Proc. 2002 IEEE/RSJ Int. Conf. Intell. Robots Syst.*, volume 3, pages 2867 – 2874, 2002.

[17] R. Mahony, F. Schill, P. Corke, and Y. S. Oh. A new framework for force feedback teleoperation of robotic vehicles based on optical flow. In *Proc. 2009 IEEE Int. Conf. Robot. and Autom.*, pages 1079 –1085, may 2009.

[18] A. Y. Mersha, A. Ruesch, S. Stramigioli, and R. Carloni. A contribution to haptic teleoperation of aerial vehicles. In *Proc. 2012 IEEE/RSJ Int. Conf. Intell. Robots Syst.*, pages 3041–3042, 2012.

[19] S. Omari, M.D. Hua, G. Ducard, and T. Hamel. Bilateral haptic teleoperation of vtol uavs. In *Proc. 2013 IEEE Int. Conf. Robot. and Autom.*, pages 2385–2391, may 2013.

[20] A. Ruesch, A. Y. Mersha, S. Stramigioli, and R. Carloni. Kinetic scrolling-based position mapping for haptic teleoperation of unmanned aerial vehicles. In *Proc. 2012 IEEE Int. Conf. Robot. and Autom.*, pages 3116 –3121, may 2012.

[21] F. Schill, X. Hou, and R. Mahony. Admittance mode framework for haptic teleoperation of hovering vehicles with unlimited workspace. In *Proc. 2010 Australian Conf. Robot. Autom.*, Dec 2010.

[22] S. Stramigioli, R. Mahony, and P. Corke. A novel approach to haptic teleoperation of aerial robot vehicles. In *Proc. 2010 IEEE Int. Conf. Robot. and Autom.*, 2010.

[23] S. Stramigioli, C. Secchi, A.J. Van Der Schaft, and C. Fantuzzi. A novel theory for sampled data system passivity. In *Proc. 2002 IEEE/RSJ Int. Conf. Intell. Robots Syst.*, volume 2, pages 1936–1941, 2002.

[24] S. Stramigioli, C Secchi, A.J. vanderSchaft, and C. Fantuzzi. Sampled data systems passivity and discrete port-hamiltonian systems. *IEEE Trans. on Robot.*, 21(4):574–587, 2005.

[25] R.Q. Van der Linde, P. Lammertse, E. Frederiksen, and B. Ruiter. The hapticmaster, a new high-performance haptic interface. In *Proc. 2002 Eurohaptics*, pages 1–5, 2002.

[26] Z. Zuo and D.J. Lee. Haptic tele-driving of a wheeled mobile robot over the internet: A pspm approach. In *Proc. 2010 IEEE Int. Conf. Decis. and Cont.*, pages 3614–3619, 2010.